minerals

MDPI

Article

The Role of ε-Fe_2O_3 Nano-Mineral and Domains in Enhancing Magnetic Coercivity: Implications for the Natural Remanent Magnetization

Seungyeol Lee and Huifang Xu *

Department of Geoscience, NASA Astrobiology Institute, University of Wisconsin—Madison, Madison, WI 53706, USA; lee572@wisc.edu

* Correspondence: hfxu@geology.wisc.edu; Tel.: +1-608-265-5887

Received: 27 January 2018; Accepted: 26 February 2018; Published: 2 March 2018

Abstract: A natural ε-Fe_2O_3 nano-mineral (luogufengite) has been discovered in young basaltic rocks around the world. Transmission electron microscopy (TEM) observed euhedral or subhedral luogufengite nano-minerals with crystal sizes ranging from 10 to 120 nm in the basaltic rocks. The magnetic property of treated scoria sample (containing 75.3(5) wt % luogufengite) showed a saturation remanence of 11.3 emu·g^{-1} with a coercive field of 0.17 tesla (T) at room temperature. Luogufengite-like nano-domains were also observed in natural permanent magnets (lodestone) and Fe-Ti oxides (ilmenite-magnetite series) with strong remanent magnetization. The structure of luogufengite-like domains (double hexagonal close-packing) is associated with the interfaces between the (111) plane of cubic magnetite and the (0001) plane of rhombohedral hematite or ilmenite. Stacking faults and twin boundaries of magnetite/maghemite can also produce the luogufengite-like domains. The nano-domains oriented along the magnetic easy axis play an essential role in enhancing the magnetic coercivity of lodestone and Fe-Ti oxide. We conclude that the luogufengite nano-minerals and nano-domains provide an explanation for coercivity and strong remanent magnetization in igneous, metamorphic rocks and even some reported Martian rocks. These nano-scaled multilayer structures extend our knowledge of magnetism and help us to understand the diverse magnetic anomalies occurring on Earth and other planetary bodies.

Keywords: luogufengite; lodestone; Fe-Ti oxide; coercivity; natural remanent magnetism

1. Introduction

Numerous studies have reported strong remanent magnetization from igneous and metamorphic rocks in the Earth's crust [1–4]. The Mars Global Surveyor spacecraft also found similar unusual remanent magnetization on the Martian crust [5,6]. The preservation of strong remanent magnetization requires high magnetic stability and coercivity. The problem is that natural remanent magnetization cannot be explained by the properties of individual magnetic minerals only because none of them are high coercivity phases [1,4,7,8].

To understand the remanent magnetic anomalies of rocks, we need to identify the mechanisms that influence their magnetic properties. Previous studies have attributed these properties to fine exsolution microstructures related to local redox conditions and slow cooling history of rock [1,2,4]. The exsolution lamellae can enhance the remanent magnetization due to magnetic coupling at the contact layers. This has been proven through natural rock samples, synthetic experiments and thermodynamic calculations [1,9–12]. However, the exact role of exsolution lamellae in enhancing the magnetic stability is still not clear.

Here, we report detailed reasons for explaining the natural remanent magnetic anomalies. A new magnetic nano-mineral of ε-Fe_2O_3 (luogufengite, IMA 2016-005) was discovered in late

Pleistocene basaltic scoria from Menan Volcanic Complex Idaho [13]. Luogufengite is a polymorph of maghemite and hematite with a large magnetic coercive field at room temperature [13,14]. In this paper, we found the luogufengite nano-minerals in other young basaltic rocks. In addition, the luogufengite-like nano-domains were found in natural permanent magnets (lodestone) and Fe-Ti oxides with high natural remanent magnetism. Our findings suggest that the unique magnetic properties of nano-minerals and nano-domains with high coercivity could explain the unusual remanent magnetization in igneous and metamorphic rocks. The observation can be an important contributor to constraints on the geomagnetic field in surface rocks of the Earth and other planets.

2. Samples

Three scoria samples and one olivine basalt with oxidized surface were collected for studying luogufengite nano-mineral: (1) Menan Volcanic Complex, Rexburg, Madison County, ID, USA [15], (2) Red Dome Lava Products Mine, Fillmore, UT, USA [16], (3) The Laguna del Maule Volcanic Field, San Clemente, Chile [17] and (4) Mauna Kea volcano, Hawaii County, HI, USA [18]. The scoria samples have a vesicular texture associated with the presence of external water during the explosive eruptions of basaltic lava (Figure 1a and Supplementary Materials Figure S1). Iron-bearing volcanic glass was oxidized to form reddish-brown iron oxide mixtures on the vesicle surfaces (Figure 1a). Lodestone samples (Supplementary Materials Figure S2) were collected from a magnetite deposit near Cedar City, UT. Hematite lamellae and micro-precipitates in the magnetite host can be seen in thin section (Figure 1b). Fe-Ti oxides (ilmenite-magnetite series) were collected from the Skaergaard layered mafic intrusion in Eastern Greenland. The early stage of coarse ilmenite exsolution lamellae with fine-scale secondary lamellae was observed in the magnetite host of the Fe-Ti oxides (Figure 1c and Supplementary Materials Figure S3).

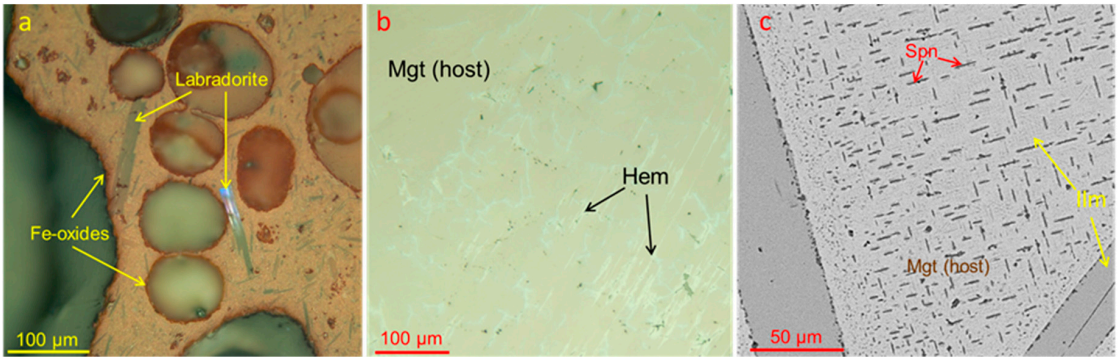

Figure 1. (**a**) A thin section of a scoria sample from the Menan volcanic Complex, Idaho under reflected light mode. The reddish Fe-oxides are coated on the vesicles' surfaces. Groundmass contains platy labradorites. (**b**) Lodestone section showing hematite (Hem) precipitates (bright) in host magnetite (Mgt). (**c**) A BSE image of a Fe-Ti oxides section showing the early stage of coarse ilmenite (Ilm) lamellae and the late stage of ilmenite exsolution lamellae with spinel (Spn) in host magnetite.

3. Experimental Methods

3.1. Enrichment of Luogufengite

The samples were carefully scratched off from the vesicles' surfaces on the collected basaltic scoria. These samples were placed in a 10 M NaOH solution at 80 °C for 2 days to remove silicate glass, following the previous procedures of synthetic ε-Fe_2O_3 [13,19]. After washing the powder with distilled water several times, the luogufengite crystals were collected by using a weak magnetic bar, separating non-magnetic minerals (hematite and silicate minerals) from the magnetic minerals. The luogufengite was further enriched by using an iron needle to pick up magnetized crystals with strong remanent magnetism. The luogufengite nano-crystals are preferentially attached to the iron

needle due to their the remanent magnetic property. These magnetic enrichment steps were repeated 5–7 times to enrich the concentration of luogufengite nano-mineral. However, the powder sample still contains other nano-minerals (nano-sized hematite, maghemite and valleyite) (Figure 2a).

3.2. Techniques

We acquired XRD results from powdered samples placed inside Kapton tubes. XRD data were collected on a 2-D image-plate detector (Rigaku, Tokyo, Japan) using a Rigaku Rapid II instrument (Mo-Kα radiation) in the Geoscience Department at the University of Wisconsin-Madison. Two-dimensional diffraction patterns were converted to conventional 2θ vs. intensity XRD powder patterns using the Rigaku 2DP software (Rigaku, Tokyo, Japan). The quantitative ratios of mineral phases were calculated with the Rietveld refinement method by using TOPAS 5 software (Bruker AXS, Madison, WI, USA). A pseudo-Voigt method was used for fitting the peak profiles. Scanning electron microscope (SEM) (Hitachi, Tokyo, Japan) analysis samples were mounted onto glass slides, polished and coated with carbon (~200 nm). All SEM images were obtained using a Hitachi S3400N variable pressure microscope with an X-ray energy-dispersive spectroscopy (EDS) (Thermo Fisher Scientific, Waltham, MA, USA) system in the Geoscience Department at the University of Wisconsin-Madison. The bright-field transmission electron microscopy (TEM) images, high-resolution TEM (HRTEM) images and selected-area electron diffraction (SAED) patterns were obtained using a Philips CM200-UT microscope operated (Philips, Amsterdam, The Netherlands) at 200 kV in the Materials Science Center at the University of Wisconsin-Madison. TEM samples were prepared both by depositing a suspension of crushed grains on a lacy carbon-coated TEM Cu-grids. Ion milled TEM sample was prepared by using a Fischione 1050 ion milling system. Magnetic hysteresis loops were measured by using a superconducting quantum interference device (SQUID) MPMS3 magnetometer Design (Quantum Design, San Diego, CA, USA) in the Chemistry Department at the University of Wisconsin-Madison. The powder and rock samples were measured with applied magnetic fields between −2 T (Tesla) and 2 T at room temperature.

4. Results and Discussion

4.1. Luogufengite Nano-Mineral with Giant Coercive Field

Luogufengite was first discovered in a late Pleistocene basaltic scoria from the Menan Volcanic Complex, Idaho using synchrotron powder X-ray powder diffraction and high-resolution TEM [13]. Luogufengite is a dark brown nano-mineral of the Fe_2O_3 polymorph [13,20]. Oxidation of Fe-bearing volcanic glass resulted in the formation of luogufengite nano-minerals on the vesicle surfaces of scoria associated with maghemite (γ-Fe_2O_3) and hematite (α-Fe_2O_3). Luogufengite is considered an intermediate phase between maghemite and hematite [21,22]. The phase transformations from maghemite to hematite via luogufengite are associated with size-dependent changes of structures from cubic closest packing (ABC) to doubled hexagonal packing (ABAC) to hexagonal closest packing (AB) (Supplementary Materials Figure S4) [21]. Synthetic ε-Fe_2O_3 nano-crystals are a promising magnetic material for technological applications due to its large coercive field value at room temperature that is not observed in other simple metal oxide magnets [19,22]. The large coercivity of ε-Fe_2O_3 is associated with the nonzero orbital momentum and large magneto-crystalline anisotropy in Fe^{3+} polyhedral [14,22]. Recently, synthetic ε-Fe_2O_3 was also identified in archeological black glazed Jian ware from China [23] and baked clay block from Spain [8].

Rietveld refinement analysis of the treated scoria sample from Menan complex shows 75.3(5) wt % luogufengite, 15.5(3) wt % hematite and 9.2(5) wt % valleyite (IMA 2017-026) [24] (Figure 2a). It is difficult to obtain pure luogufengite due to coexisting hematite intergrowths that form with luogufengite [19,21,22]. TEM images show that the size of luogufengite ranges from ~10 to 120 nm (Figure 3). The average size of natural luogufengite particles is ~40 nm in size (Figure 3). The luogufengite nano-mineral generally converts to the hematite polymorph once the crystal size exceeds

a value of ~120 nm [21]. However, large ε-Fe_2O_3 nanocrystals, with sizes up to ~200 nm, can be stable within a silica matrix [19,21]. In HRTEM images, the pseudo-hexagonal twin relationships and stacking faults along the *b*-direction are frequently observed in the luogufengite nano-minerals, producing complicated magnetic properties and large coercive field (Figure 3d–f and Supplementary Materials Figure S1) [14,21,25].

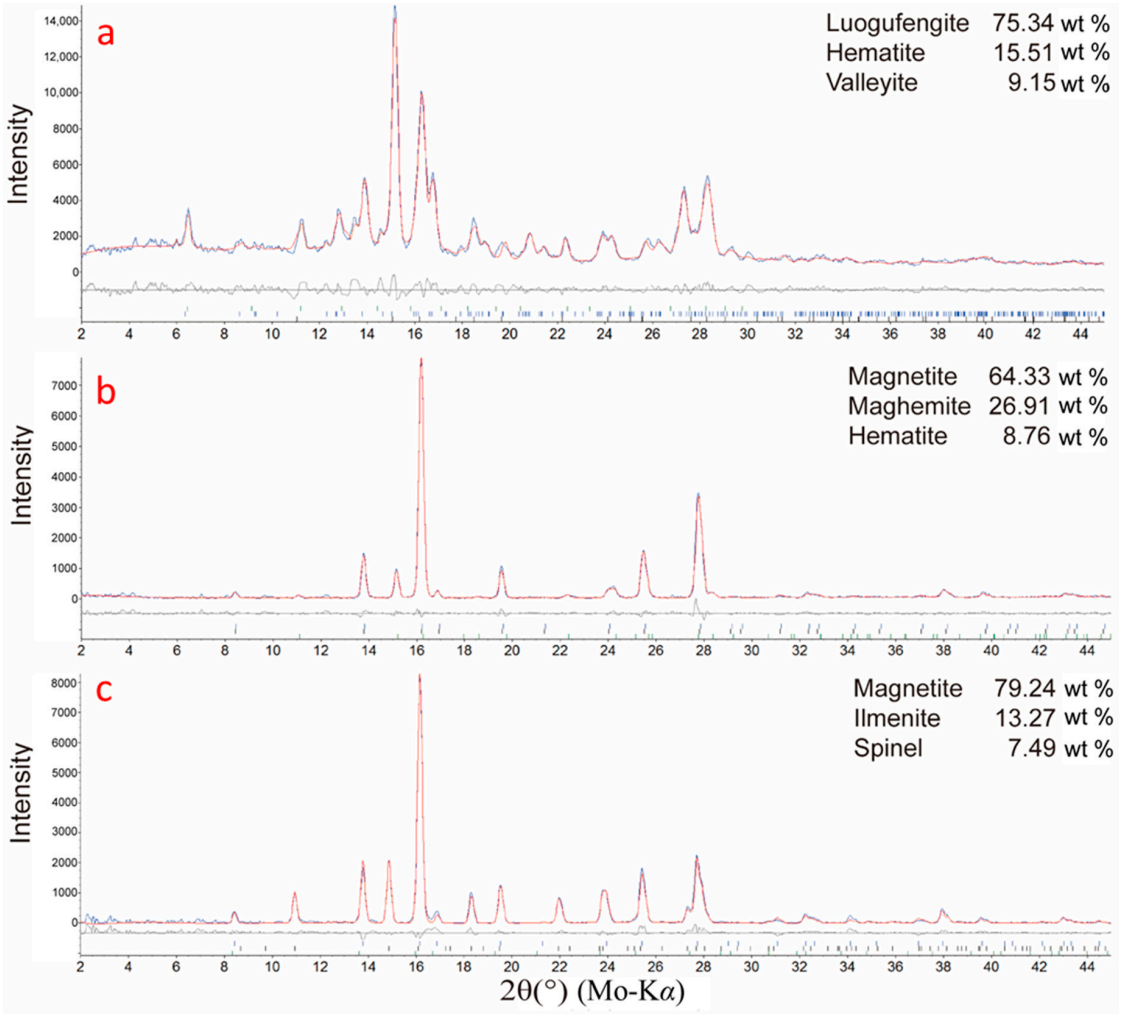

Figure 2. Powder XRD patterns of (**a**) a treated Fe-oxides sample of scoria from Menan complex, Idaho; (**b**) a lodestone sample from magnetite deposit, Utah; (**c**) a Fe-Ti oxides sample with magnetite-ilmenite series from Skaergaard layered mafic intrusion, East Greenland. Percentages of minerals were calculated by the Rietveld method with structure models [13,24,26–30].

The magnetic hysteresis loop of the treated sample (containing 75.3(5) wt % luogufengite) showed a saturation remanence of 11.3 emu·g^{-1} with a coercive field of 0.17 tesla (T) at room temperature (Figure 4). The magnetic phase of valleyite (~9.2 wt %) also influenced the hysteresis loop [24] (Figure 4). This coercivity of treated sample is significantly high compared to magnetic minerals in the earth crust [1,31]. Synthetic luogufengite had a saturation remanence of 15 emu·g^{-1} and a coercive field of 2.0 T at room temperature [19]. The coercivity of luogufengite is strongly dependent on particle size, morphology, magneto-crystalline anisotropy and cation substitution [19,22,25,32]. A rod-like morphology oriented along the *a*-axis (magnetic easy axis) has an enlarged coercive field [21–33]. A particle size of about 100 nm is the most suitable for a large coercivity to be present [19].

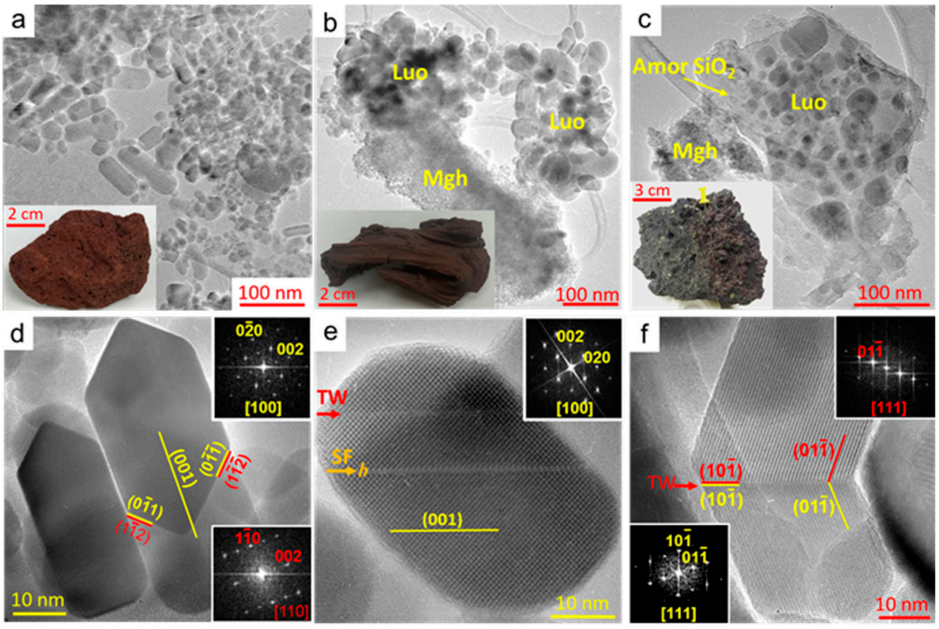

Figure 3. Hand specimens and its TEM image of iron-oxide nano-minerals (**a**) Luogufengite nano-minerals of treated samples from vesicles' surfaces on the scoria, Idaho, (**b**) Lugufengite (Luo) and maghemite (Mgh) from Fillmore scoria, Utah, (**c**) Luogufengite nano-minerals in the matrix of amorphous SiO_2 from brown surface of a Hawaii basalt, (**d**–**f**) High resolution TEM images with the fast Fourier transform (FFT) patterns of luogufengite grains showing the twinning (TW) boundaries and stacking fault (SF) along the *b*-direction.

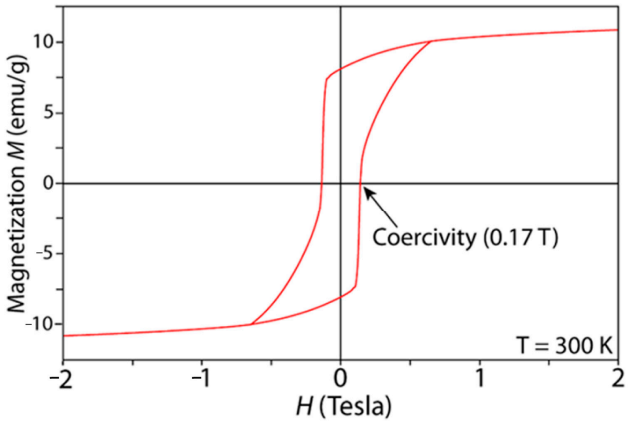

Figure 4. Magnetic hysteresis curves of the treated sample of scoria from Menan complex, Idaho.

Luogufengite nano-minerals were found in other young basaltic rocks from Red Dome in Fillmore, Utah, Laguna del Maule volcano field, Chile and on the surface of basaltic lava from Mauna Kea volcano, HI (Figure 3b,c and Supplementary Materials Figure S1). This observation suggests that the luogufengite is a widely distributed magnetic mineral in high-temperature volcanic rocks. The sizes and shapes observed in these other luogufengite nano-minerals are similar to that from Menan Volcanic Complex [13]. Luogufengite could be an important mineral for recording paleomagnetism of volcanic rocks. Its large magnetic coercivity allows for preservation of the original magnetic field during mineral formation and cooling.

4.2. Luogufengite-Like Nano-Domains in Lodestone and Fe-Ti Oxides

Many studies have revealed that exsolution lamellae are an important contributor to the unusual remanent magnetization in slow cooling igneous and metamorphic rocks [1,2,4,12]. However, the role of exsolution lamellae for the coercivity and remanent magnetization is not well understood. To understand these unusual magnetic properties, we examined lodestone and Fe-Ti oxide (ilmenite-magnetite series).

The lodestone sample analyzed (Figure 1b and Supplementary Materials Figure S2) is a natural permanent magnet. It has partially oxidized magnetite intergrown with hematite and maghemite [34,35]. Rietveld refinement analysis of a hematite-bearing lodestone shows 64.3(4) wt % of magnetite with 26.9(3) wt % of maghemite and 8.7(4) wt % of hematite (Figure 2b). Interestingly, TEM images show aligned nanoscale exsolution lamellae of hematite and magnetite (Figure 5a). HRTEM images show the interfaces $\{111\}_{Mgt}//(0001)_{Hem}$ of the nano-lamellae (Figure 5b). Many previous studies reported that this is the common interface between cubic magnetite and rhombohedral hematite, followed by oxygen packing direction of both iron oxides [1,10]. Another interesting observation of the TEM image is that host magnetite often shows stacking faults and twin boundaries related to {101} planes at the [111]-zone-axis (Figure 6a,b).

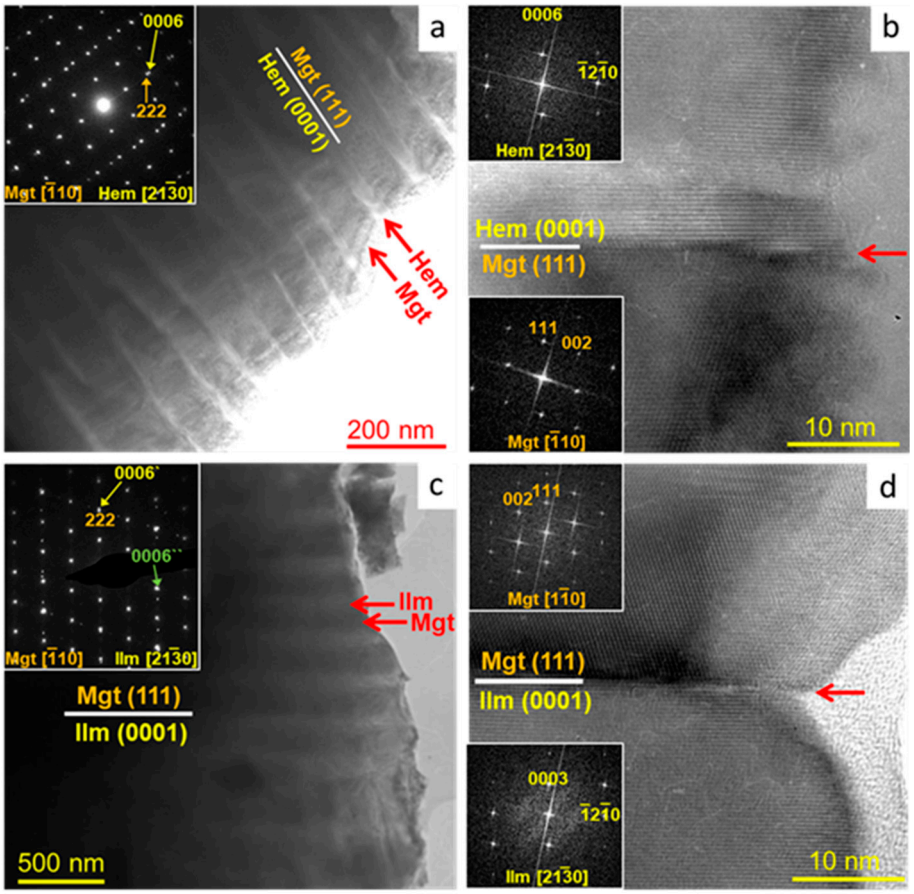

Figure 5. TEM images with the selected-area electron diffraction (SAED) patterns: (**a**) Bright-field TEM image of lodestone showing the aligned hematite (Hem) exsolution within the host magnetite (Mgt) with the $(111)_{Mgt}//(0001)_{Hem}$ interface, (**b**) High-resolution image of the magnetite-hematite interface from Figure 5a, (**c**) Bright-field TEM image of Fe-Ti oxide sample showing aligned ilmenite (Ilm) exsolution lamellae within host magnetite with the $(111)_{Mgt}//(0001)_{Ilm}$ interface. Its SAED shows the hexagonal twin relationship of ilmenite phases and (**d**) High-resolution image of the magnetite-ilmenite interface from Figure 5c.

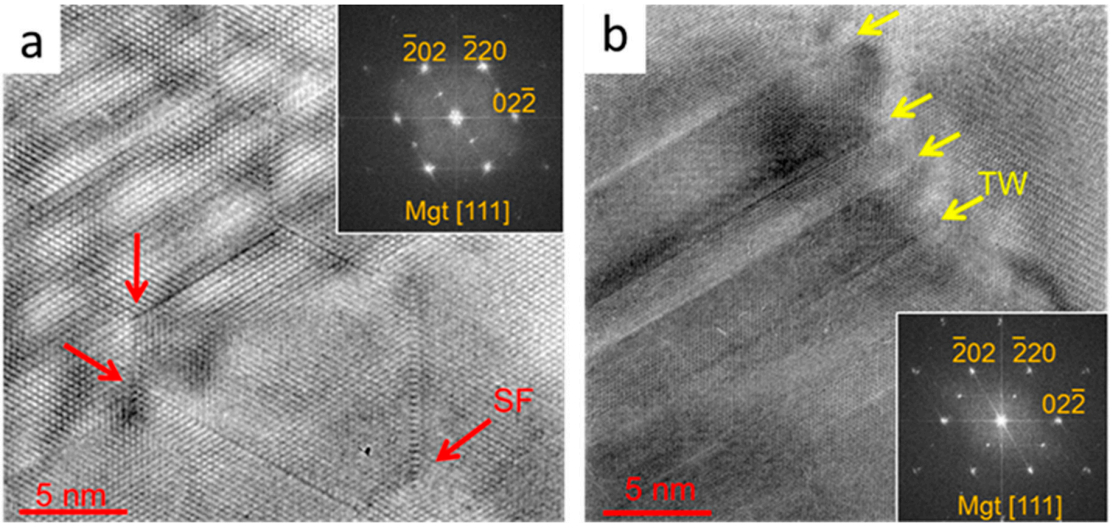

Figure 6. (**a**) High-resolution TEM image of magnetite with its FFT pattern showing the <110> displacements along [111] zone-axis. The projected displacements are associated with <111> stacking faults (SF). (**b**) High-resolution TEM image of magnetite with its FFT pattern showing twinning (TW) boundaries along [$\bar{1}$01] direction that is related to (111) twinning boundaries.

To test the interface's effect on the magnetism of lodestone, we prepared three lodestone samples with different hematite concentrations (Supplementary Materials Figure S5). Magnetic hysteresis loops from the samples clearly suggest that the magnetic coercivity is proportional to the concentration of hematite (Figure 7). The lodestone sample containing 8.7(4) wt % hematite has a coercive field of 46.7 mT at room temperature. Pure magnetite from natural rocks produced a 17.5 mT field with a grain size of 37 nm and 13.3 mT with a 100 nm grain size at room temperature [31]. From this, we can see that the interface with ABAC packing sequence enhances the coercivity field of lodestone since hematite has very weak ferromagnetic properties.

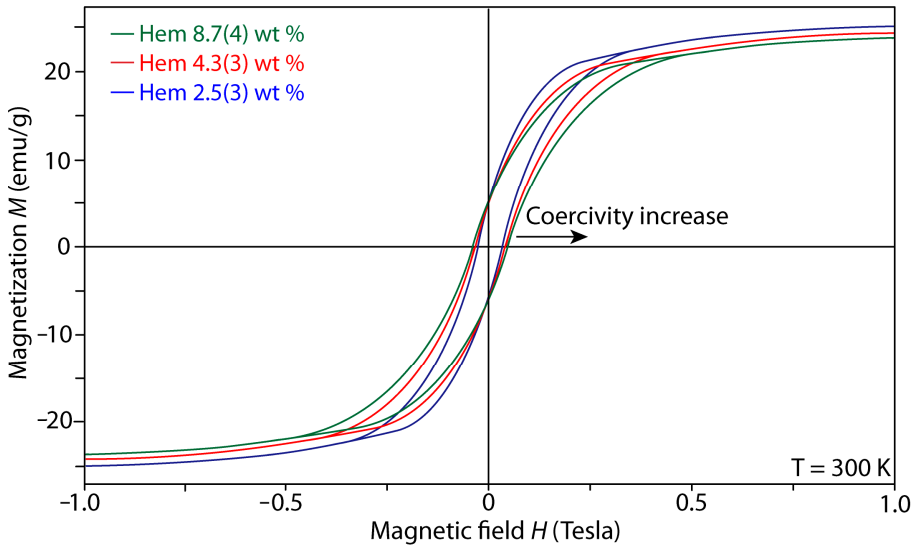

Figure 7. Magnetic hysteresis curves of three lodestone samples with different hematite concentrations at room temperature.

Ilmenite-magnetite series of Fe-Ti oxides (Figure 1c), the ilmenite exsolution lamellae in host magnetite are associated with oxidative exsolution during cooling [1,10]. Rietveld refinement analysis

of the Fe-Ti oxide sample shows 79.2(5) wt % of magnetite with the 13.3(3) wt % of ilmenite and 7.5(5) wt % of spinel (Figure 2c). Similarly, TEM images of the Fe-Ti oxide sample also show aligned lamellae of ilmenite in host magnetite, displaying an interfacial relationship of $111_{Mgt}//(0001)_{Ilm}$ (Figure 5c,d).

Previous studies have attributed natural remanent magnetization to the common interface between the (0001) planes of the rhombohedral oxide and the (111) planes of the cubic oxide [1,4,7]. Interestingly, the interface between cubic and rhombohedral oxides can produce luogufengite-like 2-D crystals or domains with a doubled hexagonal structure (ABAC packing sequence) (Figure 8a). In addition, stacking faults and twin boundaries in magnetite and maghemite can also generate luogufengite-like layer domains with the ABAC stacking sequence locally (Figure 8b,c). We suggest that the structure of luogufengite-like nano-domains at the interface or within a mineral could enhance the magnetic coercive field.

The multi-layered structure of lodestone and Fe-Ti oxides plays an essential role to enhance the coercivity and to preserve remanent magnetization (Figure 5a,c). The magnetic easy axis of luogufengite is reported to be the *a*-axis [22], which corresponds to the longitudinal axis of the multilayers of Figure 5a,c. Thus, the multi-layers are parallel to the external magnetic field that contributes to the coercive field strength [33,36]. Studies of synthetic magnetic materials have reported that the larger value of coercivity could be achieved at the interface between magnetically different layers where the multilayer materials were oriented along the magnetic easy axis [33,36,37].

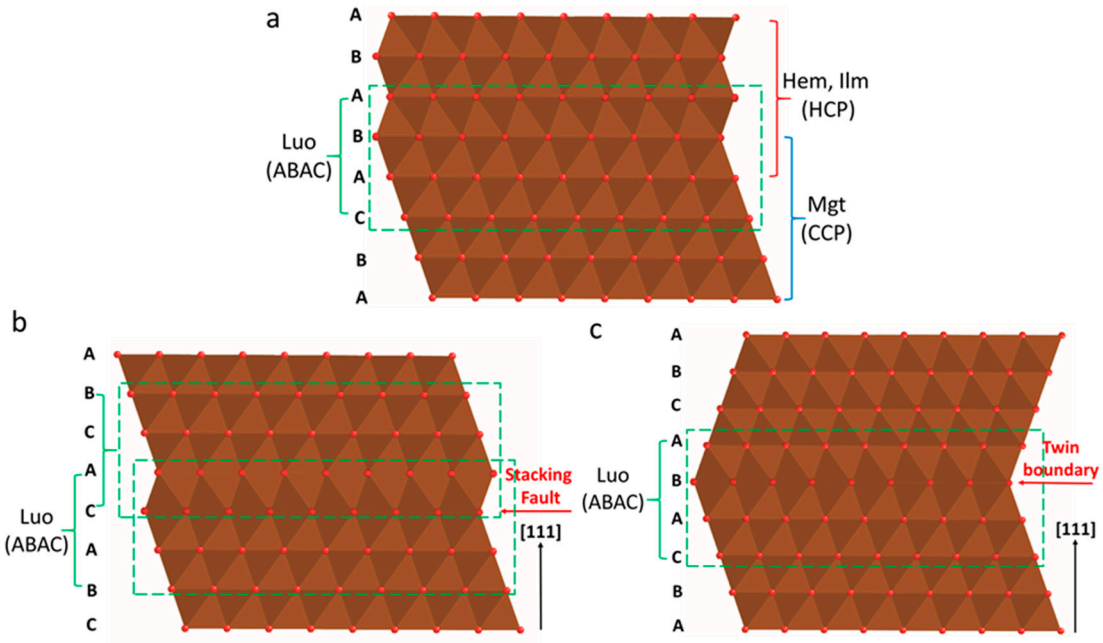

Figure 8. Structure models showing the doubled hexagonal closest packing of ABAC stacking sequence: (**a**) Crystal interface between cubic magnetite and rhombohedral hematite/ilmenite, (**b**) The (111) twin boundary of magnetite/maghemite and (**c**) The stacking fault of magnetite/maghemite along the [111] direction.

Figure 9 illustrated the nano-sized multilayer structure of lodestone and Fe-Ti oxides for understanding the coercivity and remanent magnetism. The luogufengite-like domains can be created from interfaces, twinning boundary and stacking faults along the [111] direction (oxygen packing direction) (Figure 9a). The domains/interfaces play an essential role in enhancing the magnetic coercivity of lodestone and Fe-Ti oxides (Figure 9b). The interfaces in the multi-layer texture are also associated with the magnetic coupling combined with exchange-spring state between soft and hard ferromagnets that lead to enhancing the coercive field [38,39], although the volume ratio of

luogufengite-like nano-domains at the interface is minor (Figure 9c). For example, the magnetic coercivity of the exchange-coupled isotropic FePt(hard)-Fe_3Pt(soft) nanocomposites exceeds the theoretical limit of non-exchange-coupled FePt by over 50% [40].

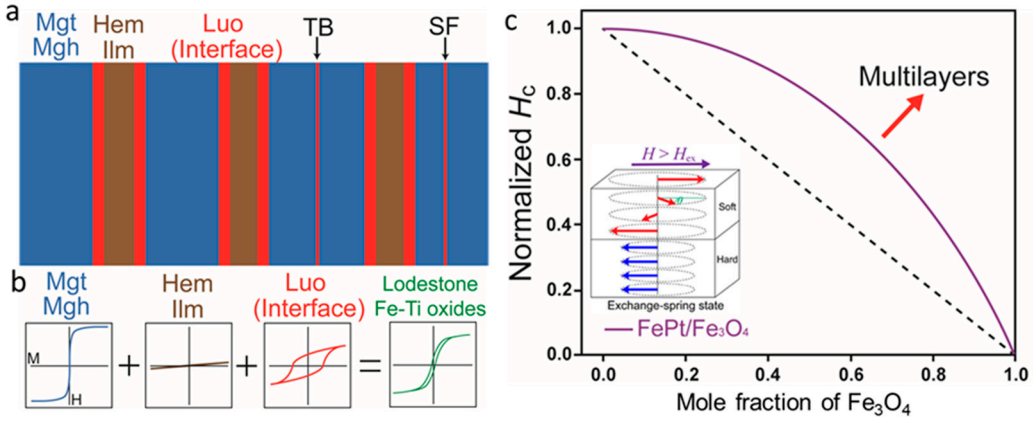

Figure 9. (**a**) Schematic diagram of multi-layer texture of lodestone and Fe-Ti oxides based on TEM observations, (**b**) Schematic diagram of *M*-*H* hysteresis loops of individual oxide minerals with the magnetic hysteresis loops of lodestone and Fe-Ti oxides, (**c**) Normalized coercive field of FePt/Fe_3O_4 core-shell nanoparticles as a function of the Fe_3O_4 mole fraction. The exchange-spring state at the interface enhances the coercivity field. TB: twin boundary and SF: stacking fault.

The paleomagnetism requires long relaxation time that retains the magnetization over geological time-scale. The relaxation time is generally proportional to the coercivity and saturation magnetization [41,42]. The relaxation times and magnetic properties can be also changed as a function of domain states and size [42]. The relaxation time of multi-domain grains increases with decreasing grain size, while that of single-domain increases with increasing grain size [41,42]. Thus, the nano-scaled multilayer structure of lodestone and Fe-Ti oxides can increase coercivity and help to preserve the saturated magnetization of rocks with the long relaxation time.

NASA's Mars Global Surveyor spacecraft observed the localized magnetic anomalies on the Mars surface [5]. Especially, Noachian crust (3.7–4.1 Ga) of the southern hemisphere of Mars shows the strongest remanent magnetism in some locations ~20 times greater than Earth, although Mars currently does not possess a core dynamo [43,44]. The candidate minerals responsible for the strong remanent magnetism on the Mars surface are magnetite, pyrrhotite, multidomain hematite, titanohematite and hemoilmenite [45,46]. We suggest that the luogufengite could be a magnetic phase in the basaltic crust on Mars. In addition, the interface, stacking faults and twinning boundary of magnetic minerals may contribute to preserving the natural remanent magnetization on Mars surface.

5. Conclusions

A natural ε-Fe_2O_3 nano-mineral (luogufengite) with large coercivity was found in young basaltic rocks. Our observations suggest that luogufengite is a widely distributed magnetic mineral in high-temperature volcanic rocks. We think that this nano-mineral can be an important indicator of paleomagnetism in volcanic systems. Luogufengite-like nano-domains were also observed at the interfaces in lodestone and Fe-Ti oxide with strong coercivity and remanent magnetization. The multilayer of nano-texture paralleled to the magnetic easy axis plays an important role in enhancing the magnetic coercivity. Stacking faults and twin boundaries can also produce luogufengite-like layer domains to help to increase the coercivity. These observations can provide an explanation for coercivity and strong remanent magnetization in slow cooling igneous and metamorphic rocks. We believe that this is a good example of using the nanostructure to describe distinctive mineral properties in natural

systems. The observation of nano-minerals and nano-domains certainly helps us to better understand anomalous magnetic properties found on Earth and other planetary systems.

Supplementary Materials: The following are available online at http://www.mdpi.com/2075-163X/8/3/97/s1, Figure S1: Images of hand specimen and the TEM images, Figure S2: Hand sample of lodestone, Figure S3: BSE image of ilmenite-magnetite series of Fe-Ti oxides, Figure S4: A size-dependent phase map of iron (III) oxide polymorphs of maghemite, luogufengite and hematite, Figure S5: Three powder XRD patterns of lodestone with different hematite concentrations, Table S1: Atomic coordinates of luogufengite.

Acknowledgments: This research was funded by the National Science Foundation and NASA Astrobiology Institute (NNA13AA94A). Authors thank Franklin Hobbs and the anonymous reviewers for their constructive suggestions.

Author Contributions: Huifang Xu conceived the idea and selected the samples; Seungyeol Lee conducted the experiments and drafted the manuscript. Seungyeol Lee and Huifang Xu analyzed the data and worked on manuscript writing.

Conflicts of Interest: The authors declare no conflict of interest.

References

1. Robinson, P.; McEnroe, S.A.; Miyajima, N.; Fabian, K.; Church, N. Remanent magnetization, magnetic coupling and interface ionic configurations of intergrown rhombohedral and cubic Fe-Ti oxides: A short survey. *Am. Mineral.* **2016**, *101*, 518–530. [CrossRef]
2. Robinson, P.; Harrison, R.J.; McEnroe, S.A.; Hargraves, R.B. Lamellar magnetism in the haematite-ilmenite series as an explanation for strong remanent magnetization. *Nature* **2002**, *418*, 517–520. [CrossRef] [PubMed]
3. McCammon, C.A.; McEnroe, S.A.; Robinson, P.; Fabian, K.; Burton, B.P. High efficiency of natural lamellar remanent magnetisation in single grains of ilmeno-hematite calculated using mossbauer spectroscopy. *Earth Planet. Sci. Lett.* **2009**, *288*, 268–278. [CrossRef]
4. McEnroe, S.A.; Fabian, K.; Robinson, P.; Gaina, C.; Brown, L.L. Crustal magnetism, lamellar magnetism and rocks that remember. *Elements* **2009**, *5*, 241–246. [CrossRef]
5. Acuna, M.H.; Connerney, J.E.P.; Wasilewski, P.; Lin, R.P.; Anderson, K.A.; Carlson, C.W.; McFadden, J.; Curtis, D.W.; Mitchell, D.; Reme, H.; et al. Magnetic field and plasma observations at Mars: Initial results of the mars global surveyor mission. *Science* **1998**, *279*, 1676–1680. [PubMed]
6. Connerney, J.E.P.; Acuna, M.H.; Ness, N.F.; Spohn, T.; Schubert, G. Mars crustal magnetism. *Space Sci. Rev.* **2004**, *111*, 1–32. [CrossRef]
7. Fabian, K.; McEnroe, S.A.; Robinson, P.; Shcherbakov, V.P. Exchange bias identifies lamellar magnetism as the origin of the natural remanent magnetization in titanohematite with ilmenite exsolution from Modum, Norway. *Earth Planet. Sci. Lett.* **2008**, *268*, 339–353. [CrossRef]
8. Lopez-Sanchez, J.; McIntosh, G.; Osete, M.L.; del Campo, A.; Villalain, J.J.; Perez, L.; Kovacheva, M.; de la Fuente, O.R. Epsilon iron oxide: Origin of the high coercivity stable low curie temperature magnetic phase found in heated archeological materials. *Geochem. Geophys. Geosyst.* **2017**, *18*, 2646–2656. [CrossRef]
9. Fabian, K.; Shcherbakov, V.P.; McEnroe, S.A.; Robinson, P.; Burton, B.P. Magnetic mean-field modelling of solid solutions: Theoretical foundations and application to the hematite-ilmenite system. *Geophys. J. Int.* **2015**, *202*, 1029–1040. [CrossRef]
10. Ramdohr, P. *The Ore Minerals and Their Intergrowths*, 2nd ed.; Pergamon Press: Oxford, UK, 1980; pp. 85–110.
11. Lattard, D. Experimental-evidence for the exsolution of ilmenite from titaniferous spinel. *Am. Mineral.* **1995**, *80*, 968–981. [CrossRef]
12. McEnroe, S.A.; Robinson, P.; Miyajima, N.; Fabian, K.; Dyar, D.; Sklute, E. Lamellar magnetism and exchange bias in billion-year-old titanohematite with nanoscale ilmenite exsolution lamellae: I. Mineral and magnetic characterization. *Geophys. J. Int.* **2016**, *206*, 470–486. [CrossRef]
13. Xu, H.F.; Lee, S.; Xu, H. Luogufengite: A new nano-mineral of Fe_2O_3 polymorph with giant coercive field. *Am. Mineral.* **2017**, *102*, 711–719. [CrossRef]
14. Tseng, Y.C.; Souza-Neto, N.M.; Haskel, D.; Gich, M.; Frontera, C.; Roig, A.; Veenendaal, M.; Nogués, J. Nonzero orbital moment in high coercivity ε-Fe_2O_3 and low-temperature collapse of the magnetocrystalline anisotropy. *Phys. Rev. B* **2009**, *79*, 094404. [CrossRef]
15. Creighton, D. Menan buttes, southeastern idaho. *Centen. Field Guide* **1987**, *2*, 109–111.

16. Doelling, H.H.; Davis, F.D.; Brandt, C.J. *The Geology of Kane County, Utah: Geology, Mineral Resources, Geologic Hazards*; Utah Geological Survey: Salt Lake City, UT, USA, 1989.
17. Frey, F.A.; Gerlach, D.C.; Hickey, R.L.; Lopez-Escobar, L.; Munizaga-Villavicencio, F. Petrogenesis of the Laguna del Maule volcanic complex, Chile (36 s). *Contrib. Mineral. Petrol.* **1984**, *88*, 133–149. [CrossRef]
18. Macdonald, G.A.; Abbott, A.T.; Peterson, F.L. *Volcanoes in the Sea: The Geology of Hawaii*; University of Hawaii Press: Honolulu, HI, USA, 1983.
19. Jin, J.; Ohkoshi, S.; Hashimoto, K. Giant coercive field of nanometer-sized iron oxide. *Adv. Mater.* **2004**, *16*, 48–51. [CrossRef]
20. Xu, H.; Lee, S. Luogufengite, IMA 2016-005. CNMNC Newsletter. *Mineral. Mag.* **2016**, *80*, 691–695.
21. Lee, S.; Xu, H.F. Size-dependent phase map and phase transformation kinetics for nanometric Iron(III) oxides ($\gamma \rightarrow \varepsilon \rightarrow \alpha$). *J. Phys. Chem. C* **2016**, *120*, 13316–13322. [CrossRef]
22. Tucek, J.; Zboril, R.; Namai, A.; Ohkoshi, S. ε-Fe_2O_3: An advanced nanomaterial exhibiting giant coercive field, millimeter-wave ferromagnetic resonance and magnetoelectric coupling. *Chem. Mater.* **2010**, *22*, 6483–6505. [CrossRef]
23. Dejoie, C.; Sciau, P.; Li, W.D.; Noe, L.; Mehta, A.; Chen, K.; Luo, H.J.; Kunz, M.; Tamura, N.; Liu, Z. Learning from the past: Rare ε-Fe_2O_3 in the ancient black-glazed Jian (Tenmoku) wares. *Sci. Rep.* **2014**, *4*. [CrossRef] [PubMed]
24. Xu, H.; Lee, S.; Xu, H.; Jacobs, R.; Morgan, D. Valleyite, IMA 2017–2026. *Mineral. Mag.* **2017**, *81*, 1035.
25. Yoshikiyo, M.; Yamada, K.; Namai, A.; Ohkoshi, S. Study of the electronic structure and magnetic properties of ε-Fe_2O_3 by first-principles calculation and molecular orbital calculations. *J. Phys. Chem. C* **2012**, *116*, 8688–8691. [CrossRef]
26. Blake, R.L.; Hessevick, R.E. Refinement of hematite structure. *Am. Mineral.* **1966**, *51*, 123–129.
27. Shmakov, A.N.; Kryukova, G.N.; Tsybulya, S.V.; Chuvilin, A.L.; Solovyeva, L.P. Vacancy ordering in gamma-Fe_2O_3–Synchrotron X-ray-powder diffraction and high-resolution microscopy studies. *J. Appl. Crystallogr.* **1995**, *28*, 141–145. [CrossRef]
28. Fjellvag, H.; Gronvold, F.; Stolen, S.; Hauback, B. On the crystallographic and magnetic structures of nearly stoichiometric iron monoxide. *J. Solid State Chem.* **1996**, *124*, 52–57. [CrossRef]
29. Wechsler, B.A.; Prewitt, C.T. Crystal structure of ilmenite ($FeTiO_3$) at high temperature and high pressure. *Am. Mineral.* **1984**, *69*, 176–185.
30. Finger, L.W.; Hazen, R.M.; Hofmeister, A.M. High-pressure crystal chemistry of spinel ($MgAl_2O_4$) and magnetite (Fe_3O_4): Comparisons with silicate spinels. *Phys. Chem. Miner.* **1986**, *13*, 215–220. [CrossRef]
31. Ozdemir, O.; Dunlop, D.J.; Moskowitz, B.M. Changes in remanence, coercivity and domain state at low temperature in magnetite. *Earth Planet. Sci. Lett.* **2002**, *194*, 343–358. [CrossRef]
32. Namai, A.; Yoshikiyo, M.; Yamada, K.; Sakurai, S.; Goto, T.; Yoshida, T.; Miyazaki, T.; Nakajima, M.; Suemoto, T.; Tokoro, H.; et al. Hard magnetic ferrite with a gigantic coercivity and high frequency millimetre wave rotation. *Nat. Commun.* **2012**, *3*, 1035. [CrossRef] [PubMed]
33. Sakurai, S.; Shimoyama, J.I.; Hashimoto, K.; Ohkoshi, S.I. Large coercive field in magnetic-field oriented ε-Fe_2O_3 nanorods. *Chem. Phys. Lett.* **2008**, *458*, 333–336. [CrossRef]
34. Wasilewski, P.; Kletetschka, G. Lodestone: Natures only permanent magnet—What it is and how it gets charged. *Geophys. Res. Lett.* **1999**, *26*, 2275–2278. [CrossRef]
35. Banfield, J.F.; Wasilewski, P.J.; Veblen, D.R. Tem study of relationships between the microstructures and magnetic-properties of strongly magnetized magnetite and maghemite. *Am. Mineral.* **1994**, *79*, 654–667.
36. Gich, M.; Gazquez, J.; Roig, A.; Crespi, A.; Fontcuberta, J.; Idrobo, J.C.; Pennycook, S.J.; Varela, M.; Skumryev, V.; Varela, M. Epitaxial stabilization of ε-Fe_2O_3 (00L) thin films on $SrTiO_3$ (111). *Appl. Phys. Lett.* **2010**, *96*, 112508. [CrossRef]
37. Kirk, T.L.; Hellwig, O.; Fullerton, E.E. Coercivity mechanisms in positive exchange-biased co films and Co./Pt multilayers. *Phys. Rev. B* **2002**, *65*, 224426. [CrossRef]
38. Zeng, H.; Sun, S.H.; Li, J.; Wang, Z.L.; Liu, J.P. Tailoring magnetic properties of core/shell nanoparticles. *Appl. Phys. Lett.* **2004**, *85*, 792–794. [CrossRef]
39. Darling, S.; Bader, S. A materials chemistry perspective on nanomagnetism. *J. Mater. Chem.* **2005**, *15*, 4189–4195. [CrossRef]
40. Zeng, H.; Li, J.; Liu, J.P.; Wang, Z.L.; Sun, S. Exchange-coupled nanocomposite magnets by nanoparticle self-assembly. *Nature* **2002**, *420*, 395–398. [CrossRef] [PubMed]

41. Dunlop, D.J.; Özdemir, Ö. *Rock Magnetism: Fundamentals and Frontiers*, 3rd ed.; Cambridge University Press: Cambridge, UK, 2001; pp. 234–259.
42. Putnis, A. *An Introduction to Mineral Sciences*; Cambridge University Press: Cambridge, UK, 1992; pp. 442–444.
43. Langel, R.; Phillips, J.; Horner, R. Initial scalar magnetic anomaly map from magsat. *Geophys. Res. Lett.* **1982**, *9*, 269–272. [CrossRef]
44. Lillis, R.; Frey, H.; Manga, M. Rapid decrease in martian crustal magnetization in the Noachian era: Implications for the dynamo and climate of early mars. *Geophys. Res. Lett.* **2008**, *35*, 14203. [CrossRef]
45. Dunlop, D.J.; Arkani-Hamed, J. Magnetic minerals in the martian crust. *J. Geophys. Res. Planets* **2005**, *110*. [CrossRef]
46. Louzada, K.L.; Stewart, S.T.; Weiss, B.P.; Gattacceca, J.; Lillis, R.J.; Halekas, J.S. Impact demagnetization of the Martian crust: Current knowledge and future directions. *Earth Planet. Sci. Lett.* **2011**, *305*, 257–269. [CrossRef]